Carbohydrate Polymers 207 (2019) 775–781

Contents lists available at ScienceDirect

Carbohydrate Polymers

journal homepage: www.elsevier.com/locate/carbpol

Tuning the rheological properties of cellulosic ionogels reinforced with chitosan: The role of the deacetylation degree

M. Mar Villar-Chavero*, Juan C. Domínguez, M. Virginia Alonso, Mercedes Oliet, Francisco Rodriguez

Chemical Engineering and Materials Department, Complutense University of Madrid, Av. Complutense S/N, 28040, Madrid, Spain

ARTICLE INFO

Keywords:
Ionogel
Cellulose
Chitosan
Deacetylation degree
Reinforcement
Rheology

ABSTRACT

The rheological and thermal properties of formulated cellulosic ionogels reinforced with chitosan with 54–84% deacetylation degrees (DDs) were studied. The ionogels were stable, and the linear viscoelastic regions (LVRs) were determined. The rheological spectra of the ionogels revealed strong physical gels. Moreover, the effect of the DD on the viscoelastic properties was significant. The ionogel reinforced with chitosan with a DD of 84% exhibited the greatest viscoelastic properties (G': ~10.6 kPa, G": 20.6–1.7 kPa, and η*: 200–0.05 kPa s).

The ionogels exhibited the same glass transition temperature, which was approximately −98 °C, and a melting temperature of 40 °C. In addition, these materials were shown to be thermoreversible. This study provided basic rheological and thermal evidence that could be used to design new ionogels reinforced with chitosan with a specific DD for use as scaffolds for wound management.

1. Introduction

Ionogels are hybrid materials with a dispersed liquid phase consisting of an ionic liquid (IL) and a continuous solid phase that is organic (biopolymers, low molecular weight gelators, metallogels,etc.), inorganic (ceramics, metals, nanotubes, etc.), or a hybrid organic-inorganic compound (Le Bideau, Viau, & Vioux, 2011; Marr & Marr, 2016). Physical or chemical interactions between the solid phase and ionic liquid are important because these interactions determine the physical properties of ionogels (Marr & Marr, 2016). ILs are greatly attractive because of the possibility of tuning their properties by using different anion-cation combinations (Vioux, Viau, Volland, & Le Bideau, 2010). In addition, the use of ILs for the formulation of ionogels offers a unique combination of properties, such as thermal stability, high conductivity, and nonflammability (Marr & Marr, 2016). Currently, these gels are emerging as functional materials in different sectors, such as chemical catalysis or biocatalysis (Bothwell & Marr, 2017; Sharma & Gupta, 2016; Vittoz et al., 2018), energy production (Fan, Wei, Li, Li, & Lu, 2018; Seo & Moon, 2018), sensors or biosensors (Ghorbanizamani & Timur, 2017; Gil-González, Akyazi, Castaño, Benito-Lopez, & Morant-Miñana, 2017; Zhang, Wang, Peng, Yan, & Pan, 2018), pharmaceuticals (Brevet et al., 2016) or manufacturing of other material composites (Niroomand, Khosravani, & Younesi, 2016; Takada & Kadokawa, 2015). Polysaccharides, such as cellulose, are of great interest as a continuous phase of ionogels because of their abundance and biodegradability and biorenewability (Zhang et al., 2017). Cellulose is a polysaccharide composed of glucose units linked through β-(1–4) glycosidic linkages. This polysaccharide is usually used for the development of cellulose-based ionogels due to its well-known dissolution capability in conventional ionic liquids (Takada & Kadokawa, 2015). Furthermore, these materials show promising properties, such as transparency, flexibility, transferability, thermoreversible gelling capability, etc. (Thiemann et al., 2014). Cellulose-based ionogels have a new potential use as an ink for 3D printing since they can be used to obtain 3D structures to produce materials, such as biological scaffolds or packaging (Markstedt, Sundberg, & Gatenholm, 2014). In this case, an initial study of the viscoelastic properties of these materials (rheological behavior) is necessary to determine the viability of the formulated structures. Moreover, knowledge of the thermal properties is also necessary to determine the temperature for use.

Chitosan, a polysaccharide with a similar structure to cellulose, is a copolymer composed of *N*-acetyl-D-glucosamine (GlcNAc) units and D-glucosamine (Glc) units. The molecular weight and the deacetylation degree (DD) are the most important properties of chitosan. The DD is defined as the molar fraction of Glc units present in the polymeric chain. Accordingly, if the DD is less than 50%, the biopolymer is

* Corresponding author.
E-mail addresses: mdm.villar@ucm.es (M.M. Villar-Chavero), jucdomin@ucm.es (J.C. Domínguez), valonso@ucm.es (M.V. Alonso), moliet@ucm.es (M. Oliet), frsomol@ucm.es (F. Rodriguez).

https://doi.org/10.1016/j.carbpol.2018.12.041
Received 12 December 2018; Accepted 15 December 2018
Available online 17 December 2018
0144-8617/

referred to as chitin, and if the DD is greater than 50%, the polymer is referred to as chitosan (Chang, Tsai, Lee, & Fu, 1997). This biopolymer has good biological properties, such as antioxidant, anticholesterolemic, antimicrobial, analgesic, and hemostatic properties, among others (Dash, Chiellini, Ottenbrite, & Chiellini, 2011). In addition to its attractive biological properties, chitosan has also been shown to be a good reinforcer of different materials, such as sponges, hydrogels, waterborne polyurethane, etc. (Fangbing, Wang, Zhu, & Zhang, 2014; Fu, Wang, Chen, & Xiao, 2015; Sun et al., 2018). However, to date, there have not been any studies that used chitosan as reinforcement material for ionogels.

The aim of this study was to formulate cellulosic ionogels using 1-butyl-3-methylimidazolium chloride (BmimCl) as the ionic liquid reinforced with chitosan with different DDs and to investigate the influence of the DD on the rheological and thermal properties. This study is intended to provide the necessary basic characteristics that could be used to design potential new reinforced ionogels for use as scaffolds for wound management.

2. Material and methods

2.1. Materials

Avicel® PH-101 microcrystalline cellulose obtained from Sigma-Aldrich (degree of polymerization: 230) and 1-butyl-3-methylimidazolium chloride (BmimCl) with a purity greater than 99% mass fraction obtained from Iolitec GmbH were used for the formulation of the ionogels.

Chitosan employed as reinforcement of the ionogels were obtained by deacetylation process of chitin (*Chionoecetes opilio* supplied by G.T.C. Bio Corporation, China) using different percentages of sodium hydroxide to obtain chitosan with DDs of 54, 62, 69, 77 and 84%, as described in a previous study (Villar-Chavero, Domínguez, Alonso, Oliet, & Rodriguez, 2018).

2.2. Determination of the viscosity average molecular weight (M_v) of chitosan

The physicochemical identity of chitosan is defined by the molecular weight and the DD (Dash et al., 2011). Therefore, the variation in the viscosity average molecular weight (M_v) of the obtained chitosan was determined to be able to conduct investigations based on the DD. To determine the M_v, chitosan samples with concentrations between 0.085 and 0.46 mg/mL were prepared in 0.2 M acetic acid/0.1 M sodium acetate aqueous solution for 5 h at 60 °C in a covered glass vessel to achieve the complete dissolution of chitosan. Then, these solutions were left to stand until they reached room temperature. The M_v was estimated according to a previous study conducted by Wang, Bo, Li, and Qin (1991) through the determination of the intrinsic viscosity (η) using the Mark-Houwink equation (Eq. (1)). The η was determined by measuring the passage time using a Cannon Fenske 100 capillary viscometer in a water bath at 30 °C:

$$\eta = K \cdot M_v^{\,n} \tag{1}$$

$$K = 1.64 \cdot 10^{-30} \cdot DD^{14} \tag{2}$$

$$n = -1.02 \cdot 10^{-2} \cdot DD + 1.82 \tag{3}$$

where K and n are functions of the DD of chitosan.

2.3. Preparation of the ionogels reinforced with chitosan

The ionogels were prepared according to the following steps: conditioning of the raw materials, preparation of the ionogel matrix, incorporation of reinforcement, and a gelation process. The conditioning of raw materials consisted of removing moisture from BmimCl, cellulose and chitosan for 12 h in a vacuum oven at 40 °C.

The operating conditions for the preparation of the ionogel matrix (BmimCl and cellulose) were based on previous studies (Tran, Duri, Delneri, & Franko, 2013; Tran, Duri, & Harkins, 2013). BmimCl was placed in a glass vessel with a hermetic seal, which was inertized and heated for 10 min at 100 °C under magnetic stirring (600 rpm) until the ionic liquid was completely melted. Then, the dried cellulose was added in three doses of 2 wt.%, up to 6 wt.% (by weight of the ionic liquid). After each addition, the vessel was inertized, and the next dose was not added until the previous dose was completely dissolved. Optical microscopy images were acquired using a Zeiss Axio Scope.A1 microscope with a Zeiss AxioCam ICc 1 camera to determine the complete dissolution time of cellulose in BmimCl. The time of dissolution was 6 h after the administration of the first dose (Fig. S1).

The reinforcement material was incorporated into the matrix under the same conditions (100 °C and 600 rpm). Chitosan with a specific DD was added in three doses of 1% up to 3% (w/w of matrix) every 30 min to avoid aggregation.

The gelation process was conducted by pouring the mixture into a steel mold covered with a PET film (GoodFellow Milinex® 0.075 mm). The mold was placed in a Vötsch VCL 4006 climate chamber with a relative humidity of 40% for 5 days at 25 °C to ensure complete gelation. The process used to obtain the formulated ionogels is shown as a schematic in Fig. 1.

In this study, the obtained ionogels are denoted as Gel54, Gel62, Gel69, Gel77, and Gel84 according to the DD of the reinforcement material used in their formulations.

2.4. Rheological testing

All rheological testing was performed using an ARES rheometer (TA

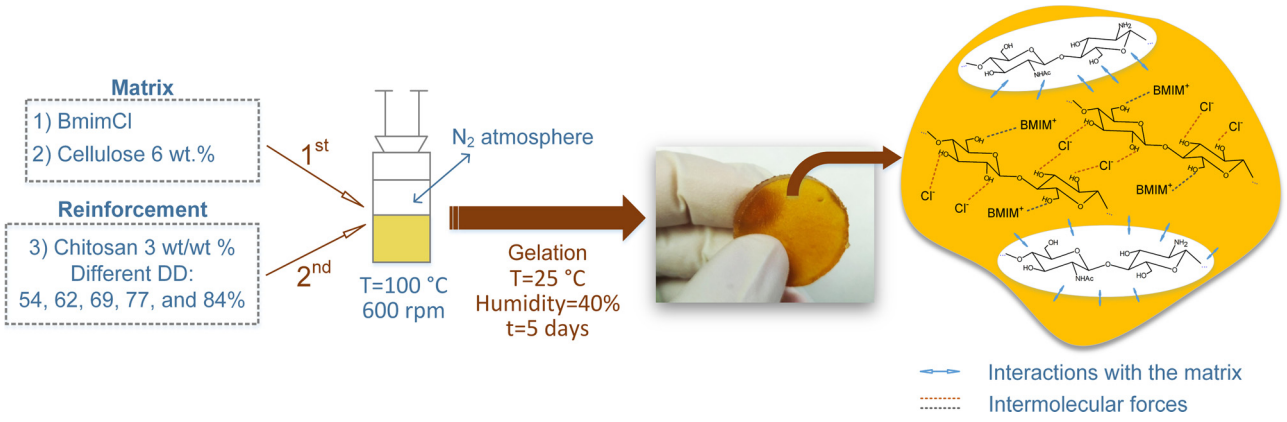

Fig. 1. Schematic of the formulation of ionogels reinforced with chitosan.

Instruments) with a 25 mm diameter serrated parallel plates geometry and a gap of 2.5 mm. Time sweep tests were performed at 25 °C with a frequency of 1 Hz and a shear strain of 0.1% for 20 min to establish the stability of the ionogels. Strain sweep tests were performed at 25 °C with a frequency of 50 Hz (the maximum frequency used to obtain the rheological spectra in the dynamic frequency sweep test) and a strain range from 0.1 to 10% to determine the linear viscoelastic region of the ionogels. Dynamic frequency sweep tests were conducted to obtain the rheological spectra at 25 °C using a frequency range from 0.01 to 50 Hz and applying a 0.5% strain (within the linear viscoelastic region).

2.5. Differential scanning calorimetry analysis

The calorimetric measurements were performed using a Mettler Toledo® 821^e differential scanning calorimetry (DSC) instrument with a medium pressure crucible (ME-26929) with a volume of 120 µL to determine the glass transition temperature (T_g) and the melting point (T_m). DSC runs were performed with three steps of the heating/cooling/heating program following the specifications of ASTM-E1356, i.e., from −140 to 130 °C using a 10 °C min^{-1} heating rate and from 130 to −140 °C using a 20 °C min^{-1} cooling rate, and both of these ramps were used to remove the thermal history of the ionogels. Finally, the measurement was conducted from −140 °C to 130 °C using a heating rate of 10 °C min^{-1}. The sample weight was between 15 and 20 mg. The DSC experiments were carried out under a nitrogen atmosphere (flow rate of 20 mL/min).

2.6. Thermoreversibility testing

Thermoreversibility testing was performed on the samples to determine whether these ionogels were reversible by the temperature (Wang, Yu et al., 2018). Therefore, the ionogels were melted for 20 min at 60 °C in a test tube to achieve complete melting. Then, the ionogels were left to stand for 1 day at room temperature to evaluate the regelation of the ionogels.

3. Results and discussion

The viscosity average molecular weights (M_vs) of the chitosans used as reinforcement of the formulated ionogels are shown in Table 1. The obtained M_vs showed a similar order of magnitude (~10^6 g/mol). For this reason, in the discussion of the present study regarding the characteristic properties of chitosan, only the DD was considered a differentiating property among the obtained chitosans.

3.1. Stability of the ionogels and the linear viscoelastic region

The stability of the ionogels was analyzed through time sweep tests using a rheometer at 25 °C. The results of these tests for the ionogels formulated with chitosan at different DDs are shown in Fig. S2. For all ionogels, the complex modulus (G^*) and the complex viscosity (η^*) remained constant over time; therefore, the samples were stable.

Furthermore, the results of the strain sweep tests for the formulated ionogels are shown in Fig. 2. The limit of the linear viscoelastic region (LVR) for samples Gel69, Gel77, and Gel84 reached a strain of 1.77%.

Table 1
Viscosity average molecular weights (M_vs) and parameters for their determination of the chitosan samples used as reinforcement materials in the ionogels.

Chitosan DD (%)	K	n	η (mL/mg)	M_v (g mol^{-1})
54	$2.86{\cdot}10^{-6}$	1.27	135	$1.09{\cdot}10^6 \pm 2.19{\cdot}10^4$
62	$1.29{\cdot}10^{-5}$	1.21	243	$1.06{\cdot}10^6 \pm 2.11{\cdot}10^4$
69	$9.09{\cdot}10^{-5}$	1.12	422	$9.38{\cdot}10^6 \pm 1.88{\cdot}10^4$
77	$5.06{\cdot}10^{-4}$	1.02	707	$9.97{\cdot}10^5 \pm 1.99{\cdot}10^4$
84	$1.45{\cdot}10^{-3}$	0.96	619	$7.10{\cdot}10^5 \pm 1.42{\cdot}10^4$

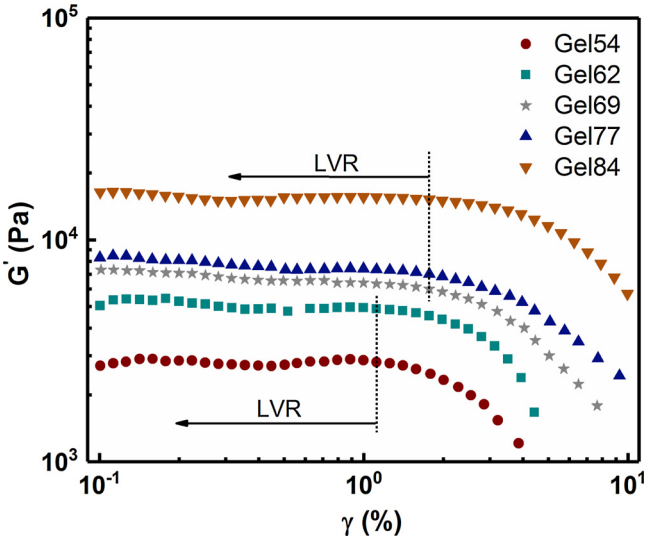

Fig. 2. Strain sweep tests for all formulated ionogels at 25 °C.

However, Gel62 and Gel54 ionogels showed the end of the LVR at a strain of 1.12%. Consequently, Gel84, Gel77, and Gel69 showed greater strength of the molecular structure than Gel62 and Gel54. In all cases, the strain applied in the dynamic frequency sweep test was within the LVR.

3.2. Rheological spectra

The rheological spectra were obtained for the formulated materials by dynamic frequency sweep tests once the stability and the linear viscoelastic region of the ionogels were determined. The elastic (G') and loss moduli (G") spectra of the reinforced ionogels are shown in Fig. 3.

The variation of the elastic and loss moduli in the rheological spectra leads to the identification of different regions according to the dominant behavior (Barnes, 2000). The spectra of the studied ionogels were located within the *plateau* region since elastic behavior was predominant in the spectrum (G' > G"), and it remained constant with the frequency in all cases. The dependence of the elastic modulus was determined by a power-law model as follows:

$$G' = G_0 \cdot \omega^a \tag{4}$$

where G_0 (Pa s^a) is a constant, which is the intercept with the log G'-axis, and a is the slope of the log G'-log frequency curve. G_0 is the gel strength, i.e., the measure of the elastic energy stored in the unit volume of the network, defined mathematically by Eq. (5) (Ranjan, Rawat, & Bohidar, 2017) as follows:

$$G_0 = \lim_{\omega \to 0} G'(\omega) \tag{5}$$

The values of the linear fitting of the spectra using Eq. (4) are shown in Table 2. The loss moduli could not be fitted because of the strong dependence at high frequency values in the spectra of the formulated ionogels.

The parameter a indicates the behavior of the gels in the *plateau* region; the closer the value of a is to 0, the greater the solid behavior (Larson, 1999). In all cases, the ionogels showed values of this parameter at approximately 0; therefore, the materials exhibited a solid-like behavior. Therefore, the formulated ionogels were classified as strong gels (Ross-Murphy, 1995). Moreover, the matrix of the studied ionogels was composed of physical interactions (Fig. 1) consisting of hydrogen bonds between −OH groups of cellulose and the anion and cation of BmimCl (Peng, Wang, Xu, & Dai, 2018), forming a physically well-structured network (strong physical gel). This was corroborated by the $(G'/G")_{mean}$ ratios, which ranged between 8.41 and 12.8 (Table 2).

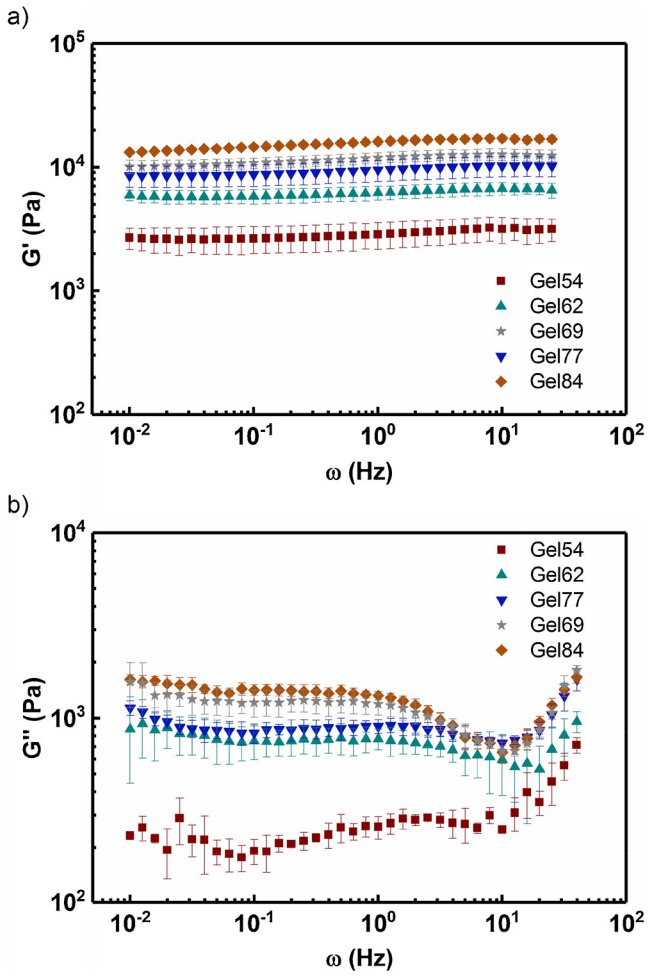

Fig. 3. Spectra of the reinforced ionogels obtained by dynamic frequency sweep tests. (a) Elastic moduli (G') and (b) loss moduli (G").

Table 2
Values of *a*, G_0 and R^2 for the correlation of $G' \sim \omega^a$, and the relation between G' and G" mean values for the formulated ionogels.

Ionogel	*a*	G_0 (Pa)	R^2	$(G'/G")_{mean}$
Gel54	0.027 ± 0.002	2887 ± 1	0.869	10.8 ± 2.3
Gel62	0.022 ± 0.001	6249 ± 1	0.892	8.41 ± 1.6
Gel69	0.034 ± 0.001	11730 ± 1	0.959	10.4 ± 3.5
Gel77	0.030 ± 0.001	9490 ± 1	0.966	10.6 ± 1.5
Gel84	0.037 ± 0.001	15831 ± 1	0.967	12.8 ± 5.1

At the same frequency, as the DD of the reinforcement material increased, both the elastic and loss moduli increased (Fig. 3a). Gel84 showed the greatest elastic behavior (~10.6 kPa), e.g., for ω = 1 Hz, the mean value of G' for Gel84 was 5.6 times greater than that of Gel54 (2.8 kPa). Similarly, the mean values of G' for Gel77, Gel69 and Gel62 were 3.3, 4 and 2.1 times greater than the value of Gel54, respectively. Therefore, the reinforcement material had an influence on the rheological properties of the ionogels, i.e., the materials acquired a more solid-like behavior by increasing the DD of the reinforcement material. Note that the G' values for Gel69 and Gel 77 overlapped, and their elastic behavior was similar.

Furthermore, the mean G" also increased as the DD of the reinforcement material increased when the frequency changed from 0.01 to 1 Hz, except in the case of Gel69, which showed loss behavior similar to Gel84 and Gel77 (Fig. 3b). These results, together with the similar elastic behavior, indicated that a DD of 69 to 77% did not influence the rheological properties of the ionogel. Gel54 exhibited the most loss behavior; for ω = 1 Hz, the G" for Gel84 was 5.1 times greater than that of Gel54 (0.26 kPa). However, at frequencies ranging from 1 to 50 Hz, all loss moduli of the formulated ionogels had the tendency to overlap (at approximately 15 Hz), i.e. they had the same viscous behavior. At frequencies greater than 15 Hz, in all cases, the values of G" increased to meet with G' in the leathery region.

The G_0 of the formulated ionogels improved when the DD of the chitosan increased (Table 2), except in the case of the G_0 of Gel69, whose value was greater than that of Gel77. However, as mentioned previously, for DDs ranging from 69 to 77%, there were no significant effects on the rheological properties. Gel84 was the ionogel with a substantial amount of elastic energy stored in the unit volume of the network, which was 81% greater than the value of Gel54.

The possible explanation for these rheological results is that chitosan with a greater DD, and therefore, a greater proportion of amine groups, has more interactions with the matrix than chitosan with a lower DD of the reinforcement material. This behavior is possible because the particles tend to restrict the movement of the matrix in the vicinity of each particle due to the hydrogen bonds between chitosan and dissolved cellulose (Li & Zhu, 2018). The greater the amount of Glc units, the greater the availability to form hydrogen bonds; thus, there is a major interaction between cellulose and chitosan (Jeffrey & Saenger, 1991). This plausible mechanism of interactions is shown in Fig. 4a, together with optical microscopy images of the homogeneity distribution of the chitosan in the cellulosic ionogel (Fig. 4b).

The ionogels demonstrated a strong dependence of the complex viscosity (η*) on the applied frequency (Fig. 5). The η* of the ionogels increased ≥84 times when the frequency changed from 0.1 to 10 Hz. This variation indicated that the obtained ionogels showed shear-thinning behavior (Larson, 1999).

The η* increased as the DD of the chitosan raised in the ionogel.

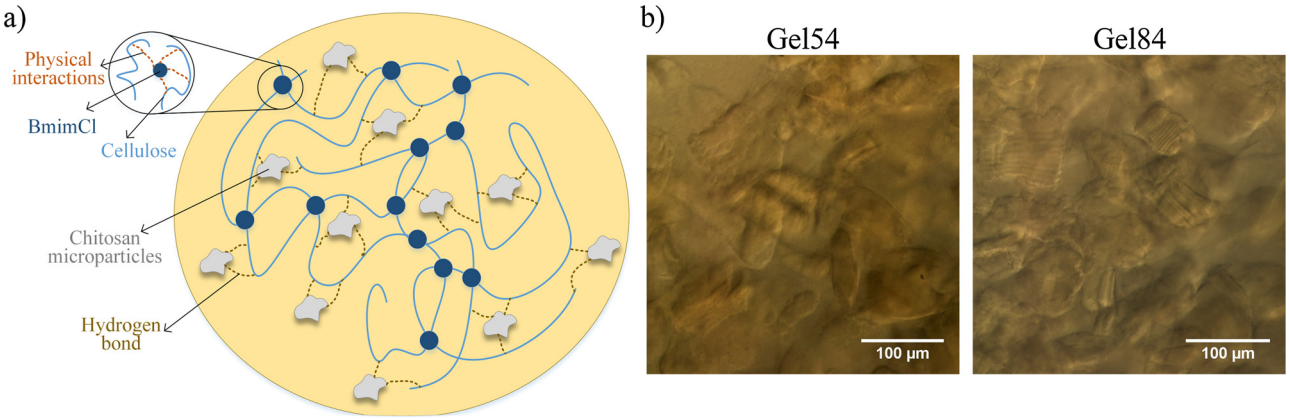

Fig. 4. (a) A schematic of plausible interactions between components in the ionogel and (b) optical microscopy images of Gel54 and Gel84.

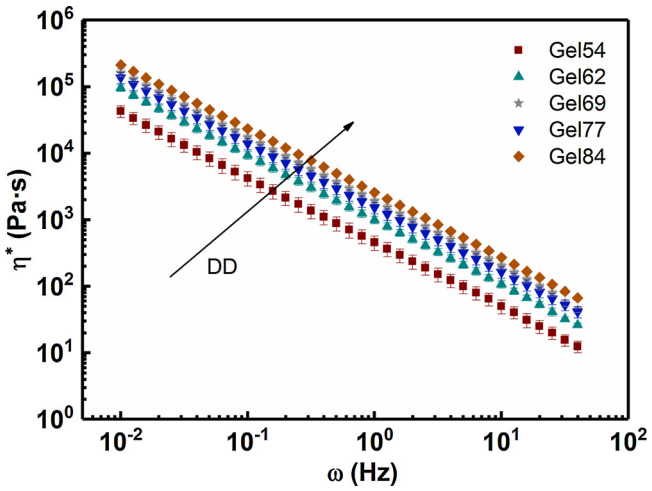

Fig. 5. Complex viscosity (η*) of the reinforced ionogels.

Therefore, Gel84 showed the greatest resistance to deformation in relation to the rest of the ionogels. For a frequency of 1 Hz, the complex viscosity values of Gel54, Gel62 and Gel78 were 82, 61 and 41%, respectively, which were less than that of Gel84. In analogy with the apparent viscosity for the viscoelastic fluids, the obtained data were fitted to the power-law model as follows:

$$\eta^* = q \cdot \omega^{p-1} \quad (6)$$

where q (Pa s^p) and p are constant parameters of the fit. The parameter q provides the resistance to deformation at frequencies near zero, and p is a measure of the slope of the log-η* vs. log-ω. The parameters of the complex viscosity fit are shown in Table 3.

The q values confirmed that as the DD of the reinforcement material increased the resistance to deformation increased, with an 82% difference between the values for Gel54 and Gel84. Similar to the results obtained for G' and G", the complex viscosity and parameter fit showed the clear influence of the DD in the interactions between the matrix and the reinforcement material of the ionogel.

Similar values of the obtained moduli (G': 2.5–10.6 kPa, G":0.15–1.7 kPa) were found for other gels with applications as medical devices. Quah, Smith, Preston, Laughlin, and Bhatia (2018) developed an alginate hydrogel that was used as a wound dressing. The alginate hydrogel presented values of G' ~8 kPa and G" between 0.12 and 1 kPa. Wang et al. (2017) developed keratin hydrogels with a G' of ~5 kPa and G" ranging from 1 to 1.1 kPa (for 20% keratin), with potential use for wound healing. Similarly, Chen et al. (2017) developed a composite hydrogel dressing with G' values between 4 and 11 kPa and G" values ranging from 0.6 to 1 kPa for 40 mg/mL gelatin microspheres. Furthermore, ionogels formulated by Trivedi, Rao, and Kumar (2014) and Sharma et al. (2015), which demonstrated solid-like behavior of physical ionogels with agarose-chitosan and agar, respectively, had similar results compared with the results obtained in this study.

Therefore, the ionogels developed in this study possess the necessary rheological properties for use as gel scaffolds for wound management. Gel84 demonstrated the best viscoelastic properties to achieve solid and strong scaffolds.

Table 3
Parameters of the power-law model of the complex viscosity of the ionogels.

Ionogel	q (Pa s^p)	p	R^2
Gel54	462 ± 1	0.028 ± 0.002	0.999
Gel62	995 ± 1	0.018 ± 0.002	0.999
Gel69	1847 ± 1	0.026 ± 0.003	0.999
Gel78	1514 ± 1	0.029 ± 0.001	0.999
Gel84	2513 ± 1	0.034 ± 0.002	0.999

3.3. Thermal properties of the ionogels

Thermal transitions of the ionogels were analyzed to investigate the influence of the reinforcement material. There are two thermal transitions shown in the thermograms in Fig. 6 as follows: glass transition and melting.

The beginning of the glass transition region for all ionogels was close to −109 °C, and the melting point (T_m) for all ionogels was approximately 40 °C. The glass transition temperatures (T_g) of Gel54, Gel62, Gel69, Gel78 and Gel84 were −98.9 ± 0.5, −98.3 ± 0.1, −97.9 ± 0.8, −98.5 ± 0.4, and −98.6 ± 0.3 °C, respectively. The difference in these values was not significant; consequently, there was no influence of the reinforcement materials on the thermal properties of the obtained ionogels. BmimCl and chitosan have glass transition temperatures of ~ (−69) °C (Fredlake, Crosthwaite, Hert, Aki, & Brennecke, 2004) and ~150 °C (Dong, Ruan, Wang, Zhao, & Bi, 2004), respectively. The obtained T_g values of the ionogels were less than that of BmimCl. This could be attributed to the water absorbed by the ionogels during the gelation step in the formulation of the ionogels since if the ionogels absorb 9% (molar) water, the T_g could be reduced up to 48 °C (Sippel et al., 2016).

Thermoreversibility testing was performed to verify that the interactions that maintained the gel-like structure were physical, consistent with the rheological properties (Fig. S3). Additionally, to check that the interactions of the reinforcement were with the dissolved cellulose, BmimCl was removed from the ionogels using water (Markstedt et al., 2014; Wang, Sun et al., 2018), and the well-structured morphology of the material was maintained (Fig. S4).

These thermal properties could allow the processing of ionogels to obtain materials by promising new techniques, such as 3D printing. Energy consumption in 3D printing could be reduced because of the low melting temperature of the ionogels (40 °C compared to 180 °C for PLA (Grémare et al., 2018), which is a standard 3D ink). Additionally, the rheological properties shown in this study were within the values reported for gel structures obtained by 3D printing: G': 5–10.5 kPa and G": 0.2–3.5 kPa (Diañez et al., 2019).

4. Conclusions

The cellulosic ionogels reinforced with chitosan with DDs between 54 and 84% were successfully developed. The rheological properties of the ionogels revealed a strong dependence with the DD of chitosan. The elastic and loss behavior, as well as the gel strength and the complex viscosity, generally increased as the DD increased because of the physical interactions between chitosan and cellulose in the ionogel (strong physical gels). Gel84 exhibited the greatest strength (81% greater than that of Gel54), with elastic and loss moduli values of 5.6 and 5.1 times greater than the values of Gel54, respectively.

In all cases, the thermal properties did not depend on the DD of chitosan since the glass transition temperature was −98 °C and the melting temperature was 40 °C. In addition, the ionogels were shown to be thermoreversible.

These results provide the preliminary foundation of the rheological and thermal properties for future studies of new biocompatible ionogels reinforced with chitosan for potential use as gel scaffolds for wound management.

Acknowledgments

This work was performed thanks to the financial support of the "Comunidad Autónoma de Madrid" (Spain) under the funded project S2013/MAE-2800, and of the "Ministerio de Ciencia, Innovación y Universidades" under the funded project CTQ2017-88623-R.

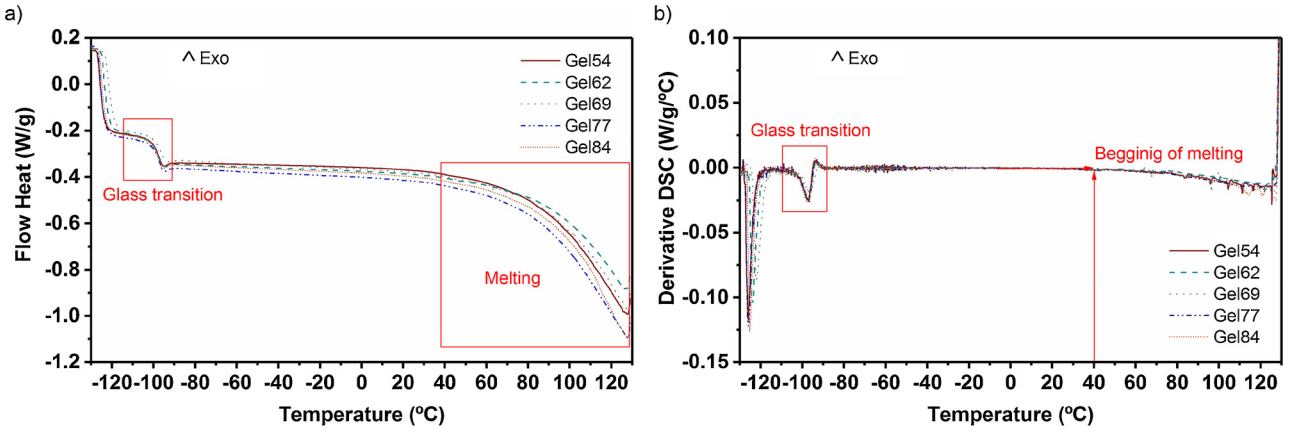

Fig. 6. (a) DSC thermograms and (b) derivative DSC of the reinforced ionogels.

Appendix A. Supplementary data

Supplementary material related to this article can be found, in the online version, at doi:https://doi.org/10.1016/j.carbpol.2018.12.041.

References

ASTM-E1356. Standard test method for assignment of the glass transition temperatures by differential scanning calorimetry.

Barnes, H. A. (2000). *A handbook of elementary rheology*. Wales, U. K: University of Wales Aberystwyth.

Bothwell, K. M., & Marr, P. C. (2017). Taming the base catalyzed sol–Gel reaction: Basic ionic liquid gels of SiO2 and TiO2. *ACS Sustainable Chemistry & Engineering, 5*(2), 1260–1263.

Brevet, D., Jouannin, C., Tourné-Péteilh, C., Devoisselle, J.-M., Vioux, A., & Viau, L. (2016). Self-encapsulation of a drug-containing ionic liquid into mesoporous silica monoliths or nanoparticles by a sol–gel process. *RSC Advances, 6*(86), 82916–82923.

Chang, K. L. B., Tsai, G., Lee, J., & Fu, W.-R. (1997). Heterogeneous N-deacetylation of chitin in alkaline solution. *Carbohydrate Research, 303*(3), 327–332.

Chen, H., Xing, X., Tan, H., Jia, Y., Zhou, T., Chen, Y., et al. (2017). Covalently antibacterial alginate-chitosan hydrogel dressing integrated gelatin microspheres containing tetracycline hydrochloride for wound healing. *Materials Science and Engineering C, 70*, 287–295.

Dash, M., Chiellini, F., Ottenbrite, R. M., & Chiellini, E. (2011). Chitosan—A versatile semi-synthetic polymer in biomedical applications. *Progress in Polymer Science, 36*(8), 981–1014.

Diañez, I., Gallegos, C., Brito-de la Fuente, E., Martínez, I., Valencia, C., Sánchez, M., et al. (2019). 3D printing in situ gelification of κ-carrageenan solutions: Effect of printing variables on the rheological response. *Food Hydrocolloids, 87*, 321–330.

Dong, Y., Ruan, Y., Wang, H., Zhao, Y., & Bi, D. (2004). Studies on glass transition temperature of chitosan with four techniques. *Journal of Applied Polymer Science, 93*(4), 1553–1558.

Fan, L., Wei, S., Li, S., Li, Q., & Lu, Y. (2018). Recent progress of the solid-state electrolytes for high-energy metal-based batteries. *Advanced Energy Materials, 8*(11), 1702657.

Fangbing, L., Wang, C., Zhu, P., & Zhang, C. (2014). Characterization of chitosan microparticles reinforced cellulose biocomposite sponges regenerated from ionic liquid. *Cellulose, 21*(6), 4405–4418.

Fredlake, C. P., Crosthwaite, J. M., Hert, D. G., Aki, S. N., & Brennecke, J. F. (2004). Thermophysical properties of imidazolium-based ionic liquids. *Journal of Chemical & Engineering Data, 49*(4), 954–964.

Fu, H., Wang, Y., Chen, W., & Xiao, J. (2015). Reinforcement of waterborne polyurethane with chitosan-modified halloysite nanotubes. *Applied Surface Science, 346*, 372–378.

Ghorbanizamani, F., & Timur, S. (2017). Ionic Liquids from biocompatibility and electrochemical aspects toward applying in biosensing devices. *Analytical Chemistry, 90*(1), 640–648.

Gil-González, N., Akyazi, T., Castaño, E., Benito-Lopez, F., & Morant-Miñana, M. (2017). Elucidating the role of the ionic liquids in the actuation behavior of thermo-responsive ionogels. *Sensors and Actuators B: Chemical, 260*, 380–387.

Grémare, A., Guduric, V., Bareille, R., Heroguez, V., Latour, S., L'heureux, N., et al. (2018). Characterization of printed PLA scaffolds for bone tissue engineering. *Journal of Biomedical Materials Research Part A, 106*(4), 887–894.

Jeffrey, G. A., & Saenger, W. (1991). *Hydrogen bonding in biological structures*. Berlin, Heidelberg: Springer-Verlag.

Larson, R. G. (1999). *The structure and rheology of complex fluids*. New York, USA: Oxford University Press.

Le Bideau, J., Viau, L., & Vioux, A. (2011). Ionogels, ionic liquid based hybrid materials. *Chemical Society Reviews, 40*(2), 907–925.

Li, G., & Zhu, F. (2018). Rheological properties in relation to molecular structure of quinoa starch. *International Journal of Biological Macromolecules, 114*, 767–775.

Markstedt, K., Sundberg, J., & Gatenholm, P. (2014). 3d bioprinting of cellulose structures from an ionic liquid. *3D Printing and Additive Manufacturing, 1*(3), 115–121.

Marr, P. C., & Marr, A. C. (2016). Ionic liquid gel materials: Applications in green and sustainable chemistry. *Green Chemistry, 18*(1), 105–128.

Niroomand, F., Khosravani, A., & Younesi, H. (2016). Fabrication and properties of cellulose-nanochitosan biocomposite film using ionic liquid. *Cellulose, 23*(2), 1311–1324.

Peng, H., Wang, S., Xu, H., & Dai, G. (2018). Preparations, properties, and formation mechanism of novel cellulose hydrogel membrane based on ionic liquid. *Journal of Applied Polymer Science, 135*(7), 45488.

Quah, S. P., Smith, A. J., Preston, A. N., Laughlin, S. T., & Bhatia, S. R. (2018). Large-area alginate/PEO-PPO-PEO hydrogels with thermoreversible rheology at physiological temperatures. *Polymer, 135*, 171–177.

Ranjan, R., Rawat, K., & Bohidar, H. (2017). Folic acid supramolecular ionogels. *Physical Chemistry Chemical Physics, 19*(34), 22934–22945.

Ross-Murphy, S. B. (1995). Structure–property relationships in food biopolymer gels and solutions. *Journal of Rheology, 39*(6), 1451–1463.

Seo, D. G., & Moon, H. C. (2018). Mechanically robust, highly ionic conductive gels based on random copolymers for bending durable electrochemical devices. *Advanced Functional Materials, 28*(14), 1706948.

Sharma, P., & Gupta, M. (2016). 1, 3, 5-Trimethylpyrazolium chloride based ionogel as an efficient and reusable heterogeneous catalyst for the synthesis of benzimidazoles. *Journal of Chemical Sciences, 128*(1), 61–65.

Sharma, A., Rawat, K., Solanki, P. R., Aswal, V., Kohlbrecher, J., & Bohidar, H. (2015). Internal structure and thermo-viscoelastic properties of agar ionogels. *Carbohydrate Polymers, 134*, 617–626.

Sippel, P., Dietrich, V., Reuter, D., Aumüller, M., Lunkenheimer, P., Loidl, A., et al. (2016). Impact of water on the charge transport of a glass-forming ionic liquid. *Journal of Molecular Liquids, 223*, 635–642.

Sun, G., Zhang, X., Bao, Z., Lang, X., Zhou, Z., Li, Y., et al. (2018). Reinforcement of thermoplastic chitosan hydrogel using chitin whiskers optimized with response surface methodology. *Carbohydrate Polymers, 189*, 280–288.

Takada, A., & Kadokawa, J.-I. (2015). Fabrication and characterization of polysaccharide ion gels with ionic liquids and their further conversion into value-added sustainable materials. *Biomolecules, 5*(1), 244–262.

Thiemann, S., Sachnov, S. J., Pettersson, F., Bollström, R., Österbacka, R., Wasserscheid, P., et al. (2014). Cellulose-based ionogels for paper electronics. *Advanced Functional Materials, 24*(5), 625–634.

Tran, C. D., Duri, S., Delneri, A., & Franko, M. (2013). Chitosan-cellulose composite materials: Preparation, characterization and application for removal of microcystin. *Journal of Hazardous Materials, 252*, 355–366.

Tran, C., Duri, S., & Harkins, A. L. (2013). Recyclable synthesis, characterization, and antimicrobial activity of chitosan-based polysaccharide composite materials. *Journal of Biomedical Materials Research Part A, 101*(8), 2248–2257.

Trivedi, T. J., Rao, K. S., & Kumar, A. (2014). Facile preparation of agarose–chitosan hybrid materials and nanocomposite ionogels using an ionic liquid via dissolution, regeneration and sol–gel transition. *Green Chemistry, 16*(1), 320–330.

Villar-Chavero, M. M., Domínguez, J. C., Alonso, M. V., Oliet, M., & Rodriguez, F. (2018). Thermal and kinetics of the degradation of chitosan with different deacetylation degrees under oxidizing atmosphere. *Thermochimica Acta, 670*, 18–26.

Vioux, A., Viau, L., Volland, S., & Le Bideau, J. (2010). Use of ionic liquids in sol-gel; ionogels and applications. *Comptes Rendus Chimie, 13*(1), 242–255.

Vittoz, P.-F., El Siblani, H., Bruma, A., Rigaud, B., Sauvage, X., Fernandez, C., et al. (2018). Insight in the alginate Pd-Ionogels. Application to the Tsuji–Trost reaction. *ACS Sustainable Chemistry & Engineering, 6*(4), 5192–5197.

Wang, W., Bo, S., Li, S., & Qin, W. (1991). Determination of the Mark-Houwink equation for chitosans with different degrees of deacetylation. *International Journal of Biological Macromolecules, 13*(5), 281–285.

Wang, J., Hao, S., Luo, T., Cheng, Z., Li, W., Gao, F., et al. (2017). Feather keratin hydrogel for wound repair: Preparation, healing effect and biocompatibility evaluation. *Colloids and Surfaces B: Biointerfaces, 149*, 341–350.

Wang, Q., Sun, J., Yao, Q., Ji, C., Liu, J., & Zhu, Q. (2018). 3D printing with cellulose

materials. *Cellulose, 25*(8), 4275–4301.
Wang, Y., Yu, Q., Bai, Y., Zhang, L., Zhou, F., Liu, W., et al. (2018). Self-constraint gel lubricants with high phase transition temperature. *ACS Sustainable Chemistry & Engineering, 6*(11), 15801–15810.
Zhang, J., Wu, J., Yu, J., Zhang, X., He, J., & Zhang, J. (2017). Application of ionic liquids for dissolving cellulose and fabricating cellulose-based materials: State of the art and future trends. *Materials Chemistry Frontiers, 1*(7), 1273–1290.
Zhang, S., Wang, F., Peng, H., Yan, J., & Pan, G. (2018). Flexible highly sensitive pressure sensor based on ionic liquid gel film. *ACS Omega, 3*(3), 3014–3021.